

Preclinical assessment of ^{68}Ga -PSMA-617 entrapped in a microemulsion delivery system for applications in prostate cancer PET/CT imaging

Vusani Mandiwana^{1,5,*}, Lonji Kalombo¹, Yolandy Lemmer¹, Philip Labuschagne¹,

Boitumelo Semete Makokotlela¹, Mike Sathekge², Thomas Ebenhan^{2,3} and Jan Rijn Zeevaart^{4,5}

¹Centre for Polymers and Composites, Council for Scientific and Industrial Research, Pretoria, South Africa

² Department of Nuclear Medicine, University of Pretoria, Pretoria, South Africa

³ Preclinical Imaging Facility, NuMeRI, Pelindaba, Pretoria, South Africa

⁴ Radiochemistry, South African Nuclear Energy Corporation, Pelindaba, Pretoria, South Africa

⁵DST/NWU, Preclinical Drug Development Platform, North West University, Potchefstroom, South Africa

* Correspondence: Vusani Mandiwana, Centre of Polymers and Composites, Council for Scientific and Industrial Research, PO Box 395, Pretoria 0001, South Africa.

Email: vmandiwana@csir.co.za

Abstract

It has in recent years been reported that microemulsion (ME) delivery systems provide an opportunity to improve the efficacy of a therapeutic agent whilst minimising side effects and also offer the advantage of favourable treatment regimens. The prostate-specific membrane antigen (PSMA) targeting agents PSMA-11 and PSMA-617, which accumulate in prostate tumours, allow for [^{68}Ga]Ga³⁺-radiolabelling and positron emission tomography/computed tomography (PET) imaging of PSMA expression in vivo. We herein report the formulation of [^{68}Ga]Ga-PSMA-617 into a ME ≤ 40 nm including its evaluation for improved cellular toxicity and in vivo biodistribution. The [^{68}Ga]Ga-PSMA-617-ME was tested in vitro for its cytotoxicity to HEK293 and PC3 cells. [^{68}Ga]Ga-PSMA-617-ME was administered intravenously in BALB/c mice followed by microPET/computed tomography (CT) imaging and ex vivo biodistribution determination. [^{68}Ga]Ga-PSMA-617-ME indicated negligible cellular toxicity at different concentrations. A statistically higher tolerance towards the [^{68}Ga]Ga-PSMA-617-ME occurred at 0.125 mg/mL by HEK293 cells compared with PC3 cells. The biodistribution in wild-type BALB/C mice showed the highest amounts of radioactivity (%ID/g) presented in the kidneys (31%) followed by the small intestine (10%) and stomach (9%); the lowest uptake was seen in the brain (0.5%). The incorporation of [^{68}Ga]Ga-PSMA-617 into ME was successfully demonstrated and resulted in a stable nontoxic formulation as evaluated by in vitro and in vivo means.

Keywords: ^{68}Ga -PSMA-617, biodistribution, in vitro, microemulsion, PET/CT, prostate cancer

1 INTRODUCTION

Prostate cancer is the most common cancer in elderly men and the second most frequent cause of cancer-related deaths (14%)¹ in western societies.² The highest incidence of prostate cancer was reported in North America and Oceania, and the lowest in Asia and Africa in 2012.³ In the United States of America, approximately 233 000 new cases and an estimated 29 480 deaths are reported annually.⁴ One of the issues of prostate cancer is early detection of recurrent disease. If the tumour is accessible for external radiation therapy or surgery, the cancer could be cured, and the resulting side effects could be delayed.⁵

Choline-based positron emission tomography/computed tomography (PET/CT) is widely used as a diagnostic imaging modality. However, numerous studies have reported low sensitivity and specificity, especially at low prostate-specific membrane antigen (PSMA) levels and high Gleason score.⁶⁻⁸ Therefore, there is a requirement for the development of new and improved imaging methods.

In this regard, an ideal biomarker, PSMA, has received significant attention as a target for imaging^{6,9} and treatment of prostate cancer.¹⁰ PSMA is a transmembrane glycoprotein hydrocellulose enzyme whose catalytic centre comprises two zinc (II) ions with a bridging hydroxide ligand¹⁰ and is also known as N-acetyl-L-aspartyl-L-glutamate peptidase.¹¹ It serves as a cell surface antigen which is overexpressed in prostate cancer cells compared with other PSMA-expressing tissues, ie, kidney, small intestines, and salivary glands.⁶ The PSMA ligand 2-[3-(1-carboxy-5-{3-naphthalen-2-yl-2-[(4-{[2-(4,7,10-tris-carboxymethyl-1,4,7,10-tetraazacyclododec-1-yl)-acetylamino]-methyl}-cyclohexanecarbonyl)-amino]-propionylamino}-pentyl)-ureido]-pentanedioic acid (PSMA-617) can be radiolabelled with the PET radioisotope Gallium-68 (⁶⁸Ga)¹ to image PSMA-expressing tumours. This PSMA ligand utilises 1,4,7,10-tetraazacyclododecane-1,4,7,10-tetraacetic acid (DOTA) as a chelating moiety which can form stable complexes with a broad range of radioisotopes such as ⁶⁸Ga, Lutetium-177 (¹⁷⁷Lu), and Yttrium-90 (⁹⁰Y) for diagnosis and therapy.¹⁰ A diagnostic or theranostic agent, consisting of three compounds, the pharmacophore PSMA, the chelator DOTA, and a radionuclide isotope, ie, ⁶⁸Ga and ¹⁷⁷Lu is often employed.

Specific cancer targeting based on low-molecular-weight radioligands may offer improved accuracy and rapid visualisation, highly effective diagnosis, and radiotherapy and improved staging. However, the dose and duration of administration of the radiopharmaceuticals are limited due to systemic toxicity and the lack of sufficient selectivity to tumour cells.⁴ There is therefore a medical need to develop drug delivery systems that selectively transport antitumour drugs or radiopharmaceuticals into the tumour cells. Delivery systems, which have demonstrated improved therapeutic index with minimal side effects, are micelles,⁴ liposomes,¹² lipid-based emulsions,¹³ and polymeric nanoparticles.⁴ The use of delivery systems such as swollen micelles or microemulsions (MEs) can improve the efficacy of a drug, allowing the total dose to be reduced and therefore minimise side effects and toxicity of the formulated compound.¹⁴

A ME is a colloidal system made out of various components including water, oil, and an amphiphile, which is optically isotropic and a dispersion of homogenous oil and water.¹⁴ MEs are translucent and form spontaneously with an average droplet diameter of 10 to 140 nm.¹⁴ They are thermodynamically stable and nanostructured.¹⁵ The advantages of MEs include improved solubility of a poorly soluble drug resulting in enhanced bioavailability of the formulated compound, protection of unstable drugs against environmental conditions, and a prolonged shelf life. The current ME was designed to formulate the drugs so that off-target delivery could be reduced by prolonging its systemic circulation time, thus, improving delivery to target. In the case of the formulated radiolabelled-PSMA-617, the prolonged circulation time aims to deliver a greater percentage of the compound to the target by slow release from the ME into the bloodstream and subsequent uptake into tissue creating a greater concentration gradient. Furthermore, the prolonged circulation and protection of the ME will reduce uptake and clearance of radiolabelled-PSMA-617 from the kidneys. Additionally, PSMA is also expressed at reduced amounts in healthy cells such as the small intestines, proximal renal tubules, kidneys, liver, and salivary glands. This means that radiation dose is delivered to these organs when [⁶⁸Ga]Ga-PSMA-617 or [¹⁷⁷Lu]Lu-PSMA-617 are used for radionuclide targeting or therapy. This has an effect on the side effect profile and safe dose that can be delivered without causing damage to nontarget tissue.¹⁶ In this study, therefore, [⁶⁸Ga]Ga-PSMA-617 was used as an imaging tool to evaluate the effect of ME on PSMA biodistribution with eventual future application for [¹⁷⁷Lu]Lu-PSMA-617. The formulation of radiopharmaceuticals into MEs offers potential prospects in the approach of diagnosing and/or treating patients with slow-release radiotherapeutics, improving their overall targeting and reducing radiation burden to vulnerable organs such as the kidneys or salivary glands.

Here, we report on the development of [⁶⁸Ga]Ga-PSMA-617-ME as a delivery system, its stability over time, its cellular toxicity to PSMA-positive PC3 and PSMA-negative HEK293 cells as well as [⁶⁸Ga]Ga-PSMA-617-ME-PET/CT imaging and biodistribution in wild-type BALB/c mice.

2 MATERIALS AND METHODS

2.1 Materials

Sodium oleate, Tween 80, polyvinyl alcohol (PVA) (97%-98% hydrolysed and Mw: 13-23 kDa), lauric acid, polyethylene glycol (PEG) 4000, and d- α -tocopherol were purchased from Sigma Aldrich (St Louis, MO, USA). HPLC-grade ethanol was purchased from Radchem Products Inc. (Orlando Park, IL, USA). All chemicals, reagents, and solvents for the radiosynthesis (ie, ultrapure, metal-free water) and analysis of the compounds were at least of analytical grade or were purchased from Sigma Aldrich (St Louis, MO, USA). PSMA-617 (C₄₉H₇₁N₉O₁₆; MW = 1042.1 g/mol) was purchased from Advanced Biochemical Compounds (Radeberg, Germany). Figure 1 shows the chemical structure of this compound including the [⁶⁸Ga]Ga³⁺-complex with DOTA.

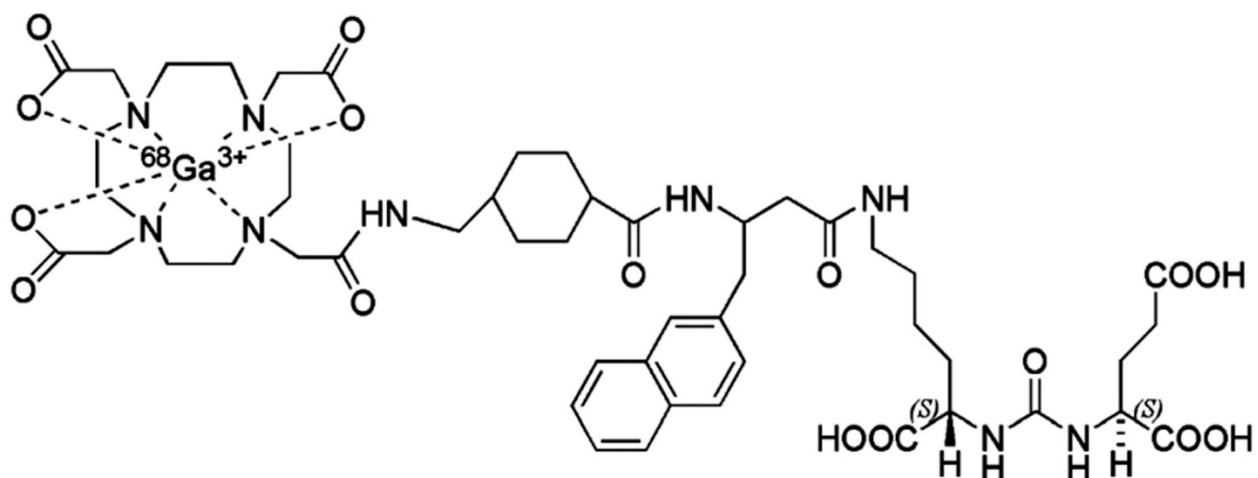


Figure 1. A schematic representation of radiolabelled ^{68}Ga -PSMA-617

2.1.1 Formulation of microemulsion

The basic ME loaded with PSMA-617 was formulated by mixing an aqueous solution of nonionic surfactant and a salt of fatty acid. Briefly, an aqueous solution of sodium oleate 0.1% w/v combined with PVA 2% w/v was prepared in volume ratio of 1:1 and mixed by stirring at room temperature. A complex of Lauric acid-PEG 4000, obtained via particles from gas saturated solution supercritical fluid process, was dissolved in ethanol whilst stirring at 75°C for 2 minutes. Tween 80, d- α -tocopherol, and PSMA-617 were added drop-wise to the organic phase, and stirring was maintained at the same heating temperature for a further 2 minutes. The resulting organic solution containing the PSMA-617 was then mixed into the PVA/sodium oleate aqueous solution at room temperature whilst maintaining stirring for 10 minutes. The resulting emulsion thereby formed spontaneously producing a translucent ME whilst cooling. Saline solution and blank ME were used as controls.

2.1.2 Characterisation of microemulsion

Particle size and size distribution indicated as the polydispersity index (PDI) were measured by dynamic laser scattering or photon correlation spectroscopy using a Malvern Zetasizer Nano ZS (Malvern Instruments, Worcestershire, United Kingdom). Each sample was measured undiluted in triplicate. The intensity-weighted mean value was measured as the average of three independent measurements. The Zeta potential was determined using a Malvern Zetasizer Nano ZS (Malvern Instruments, Worcestershire, United Kingdom) at pH 6.8 at 25°C. The instrument calculates the ME net-surface charge by determining the electrophoretic mobility using the laser doppler velocimetry. Each sample was measured undiluted in triplicate to determine the Zeta potential. The pH values of the MEs were determined at ambient temperature after a calibration process. The conductivity of the ME was measured by using a pH and conductivity meter (PC 8, Accsen, Lasec,

South Africa) at 25°C by inserting the probe into the ME. Characterisation of [⁶⁸Ga]Ga-PSMA-617 formulated into ME was performed after full decay of the radioactivity to below clearance levels.

2.2 ⁶⁸Ge/⁶⁸Ga generator elution

[⁶⁸Ga]Ga³⁺ was obtained from a SnO₂-based generator that was loaded with 1580 MBq Germanium-68 (iThemba LABS, Somerset West, South Africa). The [⁶⁸Ga]Ga³⁺ activity was manually eluted by way of an eluate-fractionation method as previously described,¹⁷ measured in a dose calibrator (CRC15, Capintec Inc, Pittsburgh, PA, USA). All radioactive measurements were corrected for decay to the time of injection. [⁶⁸Ga]Ga³⁺ (half-life 68 minutes, maximum energy of positrons [β^+]: 1.9 MeV (88%)) was obtained as [⁶⁸Ga]GaCl₃ in 2 to 3 mL of 0.6 M HCl.

2.2.1 ⁶⁸Ga-radiolabelling of PSMA-617

[⁶⁸Ga]Ga³⁺-radiolabelling of PSMA-617 was adopted from a previously described method¹⁸ making minor adaptations to manage the more acidic [⁶⁸Ga]Ga³⁺ eluate. A 2.5 M sodium acetate solution was mixed with 2 mL of [⁶⁸Ga]Ga³⁺ eluate to adjust the pH to values ranging from 3.5 to 4.5. These reaction mixtures were incubated at >95°C for 10 to 15 minutes. A Sep-Pak C18 (100 mg light) cartridge (Waters, Ireland) was used to purify the mixture from uncomplexed [⁶⁸Ga]Ga³⁺, and traces of ⁶⁸Ge which were rinsed off with saline solution. The resulting [⁶⁸Ga]Ga-PSMA-617 product was extracted from the cartridge with a 50% ethanol saline solution (v:v) and aseptically filtered using a 0.22- μ m low protein-binding membrane filter. A product sample was used to determine the radionuclidic/radiochemical identity and purity, the percentage radiochemical yield (%RCY), and percentage labelling efficiency (%LE; decay corrected).

2.2.2 HPLC and ITLC

Quality control of [⁶⁸Ga]Ga-PSMA-617 followed previously published described methods for high performance liquid chromatography (HPLC)¹⁹ and instant-thin layer chromatography (ITLC).²⁰ A reverse-phase HPLC column (Zorbax StableBond C18, 0.46 \times 2 cm \times 5 μ m; Agilent Technologies, CA, USA) performing gradient elution (5%-95% A-B over 15 minutes) at a flow rate of 1 mL/min was employed (Solvent A = 0.1% aqueous trifluoroacetic acid [TFA]; solvent B = 0.1% TFA in acetonitrile). The HPLC apparatus (Agilent 1200 series HPLC instrument, Agilent Technologies Inc., Wilmington DE, USA) combined radio-detection (GinaStar, Raytest, Straubenhardt, Germany) (counts per second) with a diode array detector following UV absorbance at 214, 220, and 240 nm. A radio-ITLC method employing a silica-gel based solid phase and 0.1 M sodium citrate as mobile phase (free [⁶⁸Ga]Ga³⁺ [R_f = 0.85] and [⁶⁸Ga]Ga-PSMA-617 [R_f = 0.2]) supported the HPLC analysis for the determination of %LE.

2.2.3 Formulation of [⁶⁸Ga]Ga-PSMA-617 into microemulsion

Similar to production and as described above, Tween 80, d- α -tocopherol, and the radiolabelled [⁶⁸Ga]Ga-PSMA-617 were added dropwise, respectively, to a lauric acid/PEG and ethanol solution and maintained stirring at a 75°C temperature for 2 minutes. The resulting organic solution containing the [⁶⁸Ga]Ga-PSMA-617 was introduced dropwise, to a PVA/sodium oleate (1:1) aqueous solution at room temperature and maintained stirring for 10 minutes. The resulting emulsion was then quenched at ambient temperature, thereby spontaneously producing a radioactive translucent ME. The specific activity for [⁶⁸Ga]Ga-PSMA-617 was in the range of 220 to 450 MBq/ μ mol. The time it took to prepare a ME containing [⁶⁸Ga]Ga-PSMA-617 ranged between 40 and 60 minutes. The radiolabelling procedure employed here was adopted from Umbricht et al,¹⁸ which would conventionally take the same amount of time. Keeping the [⁶⁸Ga]Ga-PSMA-617 radiolabelling procedure and time factor in mind, the ME formulation was designed and developed around these parameters so not to deviate from the clinical setup. It takes an additional 12 minutes to obtain the resulting ME containing [⁶⁸Ga]Ga-PSMA-617 as compared with the conventional radiolabelling of ⁶⁸Ga-PSMA-617 alone.

2.3 Cellular cytotoxicity

A WST-1 (Roche, Mannheim, Germany) colorimetric proliferation assay was used to determine the cellular toxicity of (a) the blank ME, (b) PSMA-617, (c) PSMA-617-ME, (d) [⁶⁸Ga]Ga³⁺, (e) [⁶⁸Ga]Ga-PSMA-617, and (f) [⁶⁸Ga]Ga-PSMA-617-ME. Hereby, a tetrazolium salt (WST-1 reagent) is reduced to the water-soluble orange formazan dye by cellular mitochondrial dehydrogenase in viable cells. Human prostate cancer cells (PC3, ATCC-CRL-1435, kindly provided by the Department of Biosciences, Council for Scientific and Industrial Research, South Africa) were grown in Roswell Park Memorial Institute-1640 (RPMI-1640) media (Gibco, Life Technologies, NY, USA) containing L-glutamine and supplemented with 10% foetal bovine serum. Human embryonic kidney 293 cells (HEK-293; ATCC-CRL1573, kindly provided by the ARC, Onderstepoort, South Africa) were cultured in Dulbecco modified eagle medium (DMEM) (Gibco, Life Technologies, NY, USA) containing L-glutamine and sodium pyruvate and supplemented with 10% FBS. Both cell lines were cultured at 37°C with 5% CO₂ (g) atmosphere. A density of 1 \times 10⁵ cells/mL was seeded into 96-well culture plates and allowed to adhere for 48 hours without antibiotics. Once 80% to 90% confluent, the cells were washed twice with fresh media. Serial dilutions of test compounds (a-f) in complete media were added to each well and further incubated for 24 hours. Thereafter, the cells were rinsed twice with fresh media. One hundred microliters of complete fresh media and 10 μ L of WST-1 reagent were added per well and incubated for another 2 hours at 37°C, 5% CO₂ (g) and processed as per manufacturer's instructions. Formazan absorbance was measured at a wavelength of 450 nm (against a reference wavelength of 650 nm) in a microplate reader (Tecan Infinite 500, LifeScience, PA, USA). Samples were measured in triplicates from three independent experiments.

2.4 MicroPET/CT imaging and biodistribution of [⁶⁸Ga]Ga-PSMA-617-ME

Four wild-type BALB/c mice (male, 30-40 g, 8-12 weeks old) were bred under specific pathogen-free conditions at the North West University. All experiments were approved by the North-West University Animal Care, Health and Safety Research Ethics Committee (NWU-AnimCareREC); ethics number: NWU-00333-15-A5. MicroPET/CT imaging was performed utilising small animal imaging camera (NanoScan PET/CT, Mediso Medical Systems, Hungary). Mice were immobilised on the scanner bed (orientation: prone, nose first) using a 1.5% to 2.5% isoflurane/anaesthetic air mixture for the duration of the scans and were monitored for body temperature and breathing rate. CT X-ray images were acquired for anatomical reference and to allow for scatter and attenuation correction during PET data reconstruction, using the following parameters: 50 KeV, 200 ms, 1:5 binning, and a matrix size of 125 × 125 × 125 μm. The ex vivo biodistribution study employed administration of [⁶⁸Ga]Ga-PSMA-617-ME in mice (n = 4) with the lowest injected dose of 0.76 ± 0.24 MBq and the highest injected dose of 13.96 ± 0.22 MBq. The microPET/CT imaging study employed the administration of doses ranging between 5 and 7 MBq in several mice (n = 4) with an average dose of 5.89 ± 0.64 MBq. MicroPET/CT image data were acquired at 40 and 60-minute scans. Mediso Nucline software was used for PET data reconstruction from list-mode: reconstruction algorithm 3D OSEM (six iterations), energy window 400 to 600 keV, coincidence mode 1 to 5, corrections for random events, detector normalisation, decay and dead time, and voxel size 0.6 mm. Mediso Inter View Fusion software (version 2.02.055.2010) was used for data visualisation, yielding coregistered PET/CT images in axial, coronal, and sagittal orientation. Time-activity curves yielded by semiquantification of tissue/organ tracer concentrations were analysed by way of area-under-the-curve analysis determining the normalised uptake value (SUV), which is the regional tissue radioactivity concentration normalised for the injected dose and body weight of the subject. Following microPET/CT, mice were sacrificed by cervical dislocation, and tissue/organs (blood, heart, lungs, liver, spleen, kidneys, intestines, stomach, urine, tissue, bone, and brain) were isolated, weighed, and counted in an automated gamma counter (Hidex Gamma Counter AMG, Turku, Finland). The ex vivo results were expressed as percent injected dose per gram of tissue or organ (% ID/g).

For in vivo administration of MEs, a physiological pH was desired; hence, the pH was adjusted with the addition of ~20-μL 2.5 M sodium acetate (alternatively phosphate buffered saline) successfully increasing it to pH 7.5.

2.5 Statistical analysis

All experiments were performed in triplicates or more. Quantitative data were expressed as mean ± standard deviation of mean. If applicable, values were compared using Student's *t* test. *P* values <0.05 were considered statistically significant. A Grubb's test, also called the extreme studentised deviate method, was performed to determine whether a value was a significant outlier from the rest.

3 RESULTS AND DISCUSSION

3.1 Size and Zeta potential

The physical and chemical properties of the ME were analysed, including particle size, surface charge, pH, and conductivity. These parameters have a direct impact on the stability and release kinetics of the radiopharmaceutical that was entrapped. The bigger the Zeta potential of the suspension, the more likely it is to be stable because the charged particles repel each other and therefore overcome the natural tendency to aggregate and wherein it is accepted that Zeta potentials more than ± 30 mV are sufficient for good electrostatic stabilisation.²¹ Table 1 summarises the data comparing blank ME with [⁶⁸Ga]Ga-PSMA-617-ME (n = 3).

Table 1. Characterisation of ME, [⁶⁸Ga]Ga-PSMA-617-ME, and PSMA-ME formulations

	F	Size, nm	PDI	ZP, mV	pH	Conductivity, $\mu\text{S}/\text{cm}$
ME (blank) (not buffered)	1	21.05 \pm 0.06	0.23 \pm 0.01	-26.06 \pm 0.15	6.30	12.53
	2	21.54 \pm 0.13	0.21 \pm 0.02	-28.10 \pm 3.55	6.22	13.20
	3	21.01 \pm 0.01	0.15 \pm 0.18	-28.34 \pm 0.85	6.17	13.19
[⁶⁸ Ga]Ga-PSMA-ME	4	18.30 \pm 0.08	0.21 \pm 0.00	-30.10 \pm 0.51	7.89	13.82
	5	21.15 \pm 0.26	0.30 \pm 0.00	-28.70 \pm 0.15	7.93	13.50
	6	35.77 \pm 1.38	0.64 \pm 0.04	-27.10 \pm 0.66	7.88	14.35
PSMA-ME	7	22.04 \pm 0.15	0.25 \pm 0.01	-29.43 \pm 0.40		
	8	21.84 \pm 0.08	0.24 \pm 0.00	-28.00 \pm 0.89		
	9	22.13 \pm 0.26	0.26 \pm 0.00	-28.91 \pm 0.70		

Abbreviations: F, formulation; PDI, poly dispersity index; ZP, Zeta potential.

Various parameters were optimised to obtain an average ME particle size ranging between 20 and 40 nm, with an average PDI ≤ 0.3 . Both types of ME formulations had a Zeta potential ranging between -22 and -31 mV. The stability of the ME formulations was acceptable and close to a range which is considered high (-31 mV).

For in vivo administration of MEs, a physiological pH is desired; hence, the pH was adjusted with 2.5 M sodium acetate to pH 7.5. Conductance of MEs increases as droplets tend to fuse as a result of the percolation effect, thereby allowing enhanced transportation of ions.¹⁷ Conductivity values above 0.1 mS/cm suggest that the formed MEs were of an oil-in-water (o/w) type.^{17, 22} F6 may have its high conductance as a result of the percolation effect relating to the droplet size (>21 nm) and the concentration of sodium oleate salt, which may dissociate, resulting in enhanced movement of ions. The resulting pH of blank ME was 6.23 ± 0.13 . The pH values obtained from all the formulated MEs were all ≤ 6 before buffering and approaching a neutral pH.

The conductivity increased slightly but was not significantly affected by incorporation of $[^{68}\text{Ga}]\text{Ga-PSMA-617}$. F1 had the lowest conductivity, and F6 had the highest readings. Gallium-68 was fully decayed before this analysis; hence, no difference between $[^{68}\text{Ga}]\text{Ga-PSMA-ME}$ and PSMA-ME is expected.

For the in vivo applications, F4 was selected due to the high conductivity value, a small droplet size (depicted in Figure 2), small PDI, and high integrity (see low ZP). As there was no significant difference between this formulation and the one without the $[^{68}\text{Ga}]\text{Ga-PSMA-617}$ and furthermore such formulation is radioactive, it was not tested prior to the in vivo study.

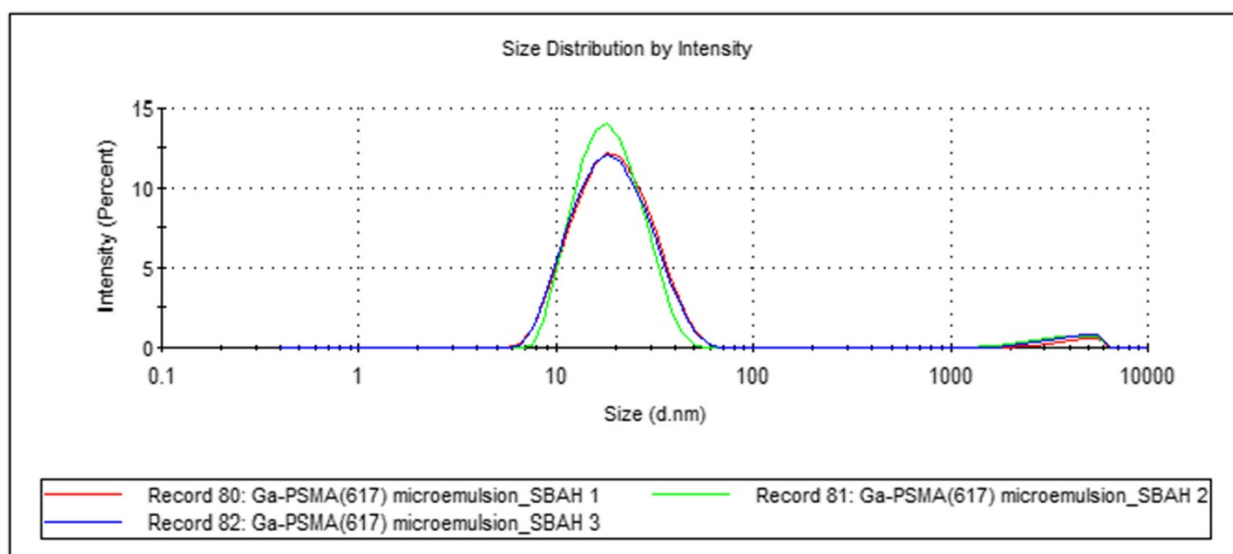


Figure 2. Graph showing the size distribution intensity of a $[^{68}\text{Ga}]\text{Ga-PSMA-617-ME}$ ($n = 3$)

3.2 Generator elution and ⁶⁸Ga-radiolabelling of PSMA-617

Eluate fractionation yielded 500 to 850 MBq (88%-92% of elutable [⁶⁸Ga]Ga³⁺ activity) in 2 mL, sufficient for straightforward radiolabelling (>99% radionuclide purity).

The optimal radiolabelling yield of [⁶⁸Ga]Ga-PSMA-617 was achieved as a function of pH (3.5-4.5) and temperature (10-15 minutes at >95°C). Further optimisations have shown that as low as 20-μg PSMA-617 was sufficient to produce a high [⁶⁸Ga]Ga-PSMA-617 yield (%LE = 98 ± 2% at pH 4 using 110-195 MBq/mL eluate; (n = 5)). The % RCY of [⁶⁸Ga]Ga-PSMA-617 was ≥97% (n = 3) based on ITLC analysis. The radioactivity for the produced [⁶⁸Ga]Ga-PSMA-617 was in the range of 220 to 450 MBq.

3.2.1 HPLC and ITLC

ME-free samples were analysed immediately after [⁶⁸Ga]Ga-PSMA-617 radiolabelling and subsequently after further 2 and 10-minute incubation at 75°C. The [⁶⁸Ga]Ga-PSMA-617 conjugate was heated to investigate the integrity of the radiolabelled product at 75°C. This was done in order to indirectly determine the fate and integrity of the conjugation of [⁶⁸Ga]Ga³⁺ to PSMA-617 at temperatures at which the ME was formulated.

The retention time of [⁶⁸Ga]Ga-PSMA-617 was 6.44 minutes, and no free [⁶⁸Ga]Ga³⁺ was detected. This was after purification of the labelled product. The radiochemical purity of the final product was 100%, and the labelling yield was 98%, shown in Figure 3.

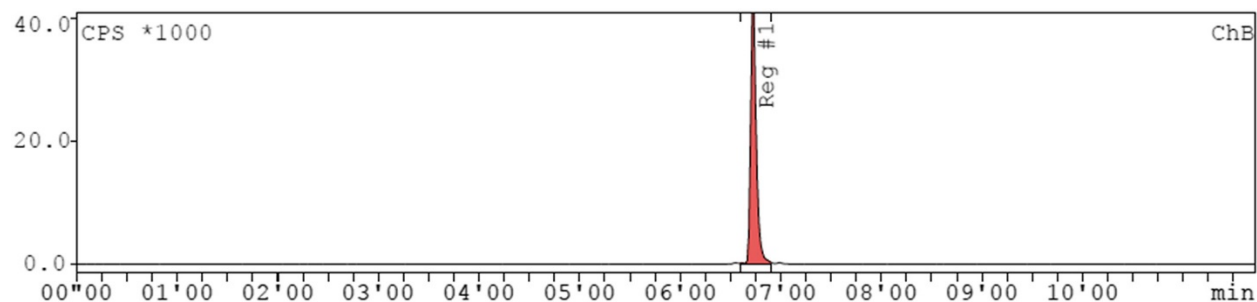


Figure 3. Radio-HPLC chromatograms of radiolabelled [⁶⁸Ga]Ga-PSMA-617

The radiochemical purity of [⁶⁸Ga]Ga-PSMA-617 remained 100% after a 2-minute incubation at 75°C. After purification, the retention time was 5.58 minutes, shown in Figure 4.

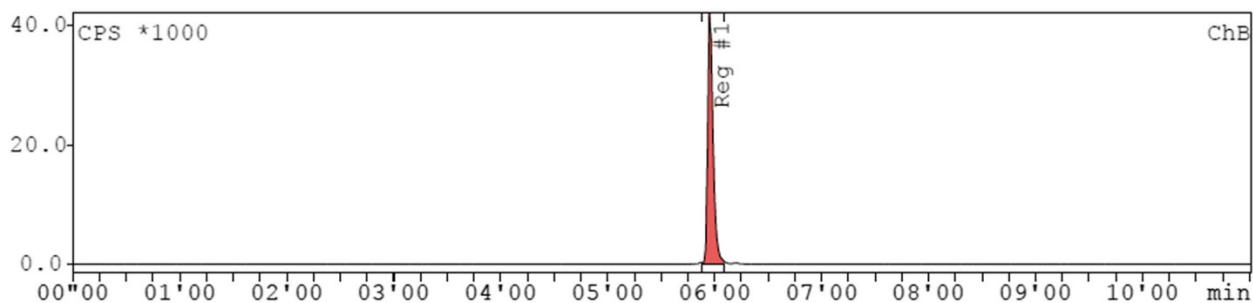


Figure 4. Radio-HPLC of $[^{68}\text{Ga}]\text{Ga-PSMA-617}$ which was heated at 75°C for 2 min postradiolabelling

The retention time after purification of the radiolabelled product was 5.58 minutes for the sample which was incubated for 10 minutes at 75°C , similar to the sample which was incubated for 2 minutes. The radiochemical purity was still 100% and therefore was not compromised at that particular temperature. No free $[^{68}\text{Ga}]\text{Ga}^{3+}$ was detected in either of the HPLC chromatograms, therefore confirming the radiosynthesis of $[^{68}\text{Ga}]\text{Ga-PSMA-617}$, as seen in Figure 5. This confirms that the $[^{68}\text{Ga}]\text{Ga-PSMA-617}$ is still intact after the ME production. Inclusion of ME does not allow for HPLC analysis due to the content and particle size. The radiochemical purity of $[^{68}\text{Ga}]\text{Ga-PSMA-617}$ was not compromised at conventional radiolabelling temperatures and at 75°C . No free $[^{68}\text{Ga}]\text{Ga}^{3+}$ was detected in either of the HPLC chromatograms. This observation therefore confirmed the radiosynthesis integrity of $[^{68}\text{Ga}]\text{Ga-PSMA-617}$. The retention time of $[^{68}\text{Ga}]\text{Ga-PSMA-617}$ was detected at slightly earlier times (5.58-6.44 minutes). This may be due to the consecutive alignment of the radio-HPLC detectors. Temperature may not have had any direct influence nor compromised the radiolabelling parameters.

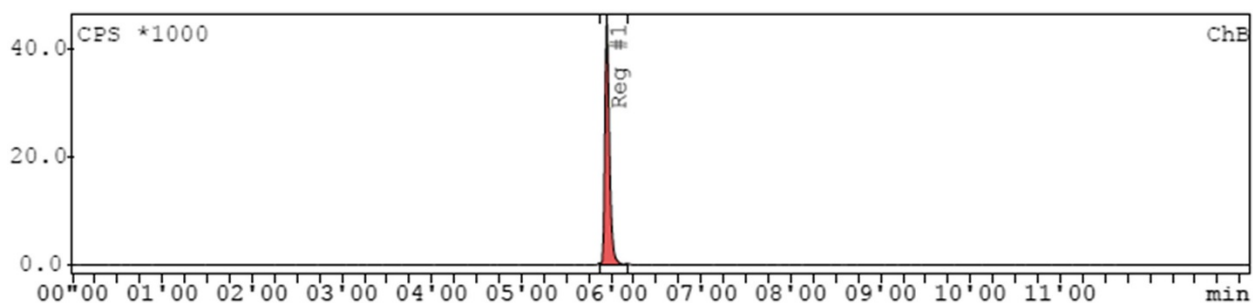


Figure 5. Radio-HPLC of $[^{68}\text{Ga}]\text{Ga-PSMA-617}$ which was heated at 75°C for 10 min postradiolabelling

3.2.2 Formulation of $[^{68}\text{Ga}]\text{Ga-PSMA-617}$ into microemulsion

Formulation was achieved as described above. The radioactivity for produced $[^{68}\text{Ga}]\text{Ga-PSMA-617-ME}$ was in the range of 220 to 450 MBq. The $[^{68}\text{Ga}]\text{Ga-PSMA-617-ME}$ s which were used for IV administration into four mice were in the size range of 21.15 ± 0.26 nm to 35.77 ± 1.38 nm, a size distribution (PDI) of 0.21 ± 0.00 to 0.64 ± 0.04 , and a Zeta potential of -28.70 ± 0.15 mV to -30.10 ± 0.51 mV, respectively. This was determined after decay of the formulation to below exclusion levels.

3.3 Cellular cytotoxicity

The in vitro cytotoxicity of the ME, PSMA-617 peptide, and the combination thereof with and without the $[^{68}\text{Ga}]\text{Ga}^{3+}$ were tested in PC3 and HEK293 cell lines. A concentration range from 1 mg/mL up to 0.0001 mg/mL was used in a WST assay over a period of 24 hours.

Free PSMA-617 in PC3 cells was considered nontoxic at concentrations lower than 0.5 mg/mL with some variations at the lower concentrations used, as similarly observed in literature.¹⁸ The ME alone showed a decrease in cell proliferation in itself and could contribute towards the cytotoxic effect of the PSMA-617 as can be seen in Figure 6. The cytotoxicity of ME indicates that there are components within the ME which affects the cell viability, but it has not been further investigated yet. The final formulation may have a synergistic effect when containing for example ^{68}Ga -PSMA-617. Li et al²³ have demonstrated that Tween 80 may affect cell assays when screening for the cytotoxicity of drugs by detecting biochemical changes on the cell membrane. The combination of the PSMA-617 and ME was more cytotoxic compared with the PSMA-617 alone at higher concentrations tested above 0.03 mg/mL but would be suitable for use at concentrations below that. Interestingly, the ME combination with PSMA-617 and $[^{68}\text{Ga}]\text{Ga}^{3+}$ (Figure 7) showed more tolerance by the cells and were less toxic at higher concentrations compared with the ME with or without PSMA-617 only (Figure 6).

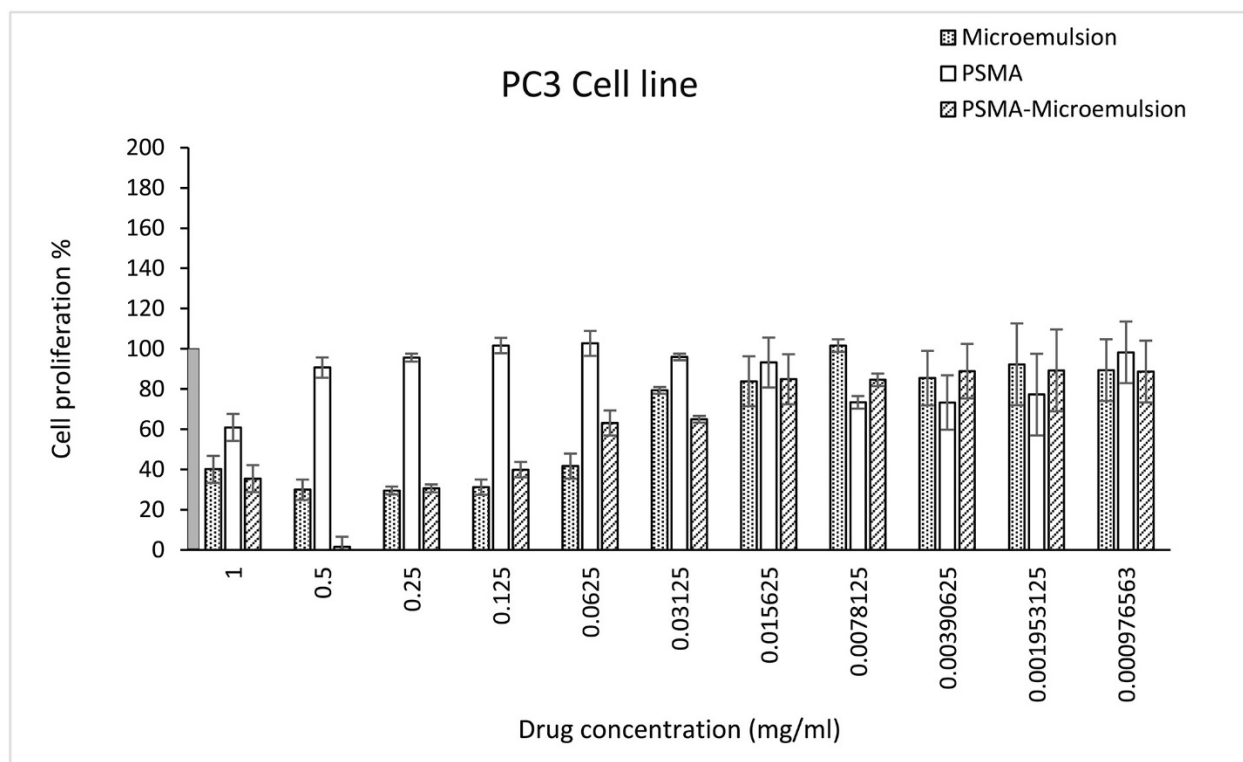


Figure 6. The in vitro cytotoxicity of a blank ME, PSMA-617, and PSMA-617 loaded ME against PC3 cells after 24 h (n = 9). Grey bar represents the untreated control cells

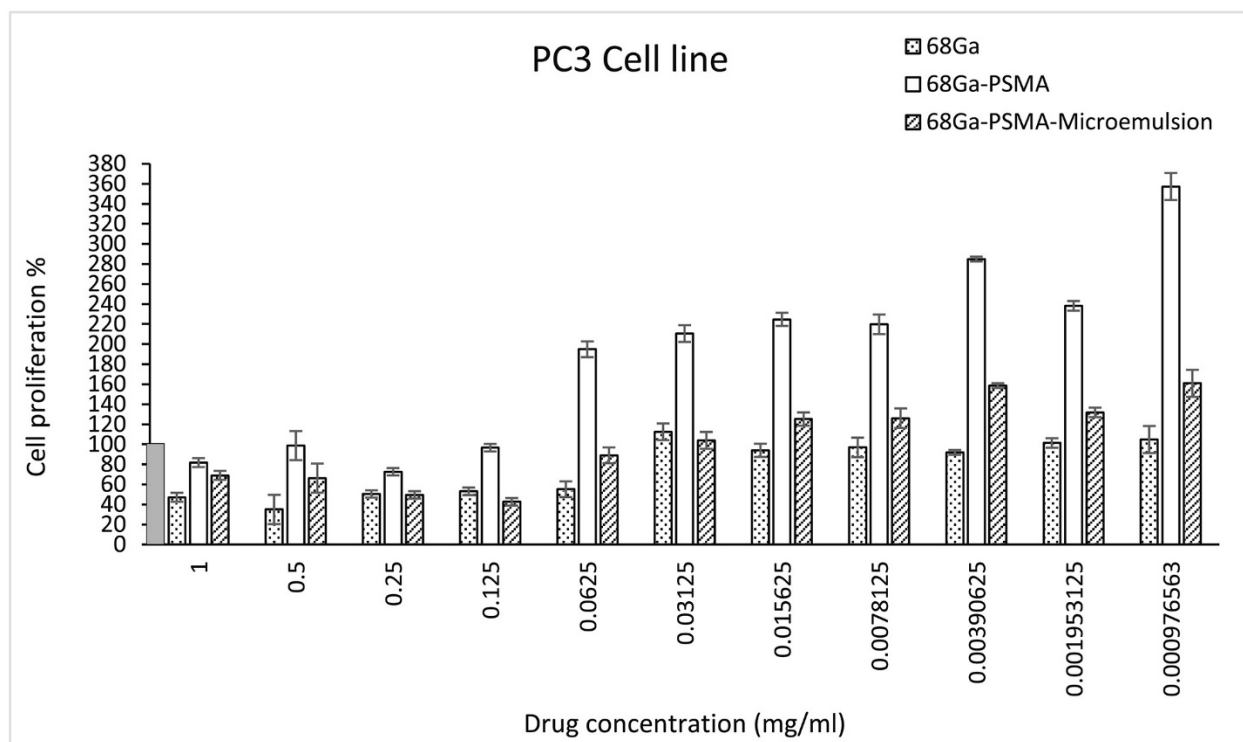


Figure 7. The in vitro cytotoxicity of $[^{68}\text{Ga}]\text{Ga}^{3+}$, $[^{68}\text{Ga}]\text{Ga-PSMA-617}$, and $[^{68}\text{Ga}]\text{Ga-PSMA-617}$ -loaded ME against PC3 cell lines after 24 h (n = 9). Grey bar represents the untreated control cells

The $[^{68}\text{Ga}]\text{Ga-PSMA-617}$ -MEs which were used for seeding into 96-well plates were in the size range of 21.15 ± 0.26 nm to 35.77 ± 1.38 nm, a PDI of 0.30 ± 0.00 to 0.64 ± 0.04 , and a Zeta potential of -28.70 ± 0.15 mV to -30.10 ± 0.51 mV, respectively. The seeded radioactivity across all the wells (1 mg/mL) was in the range of 20.00 to 30.15 MBq which was the total cumulative radioactivity across all the wells on the plate. Mean activity of 0.70 ± 0.28 MBq was seeded in 100 μL composed of complete media containing 10% FBS per well.

$[^{68}\text{Ga}]\text{Ga-PSMA-617}$ is a radiopharmaceutical peptide conjugate which is used to diagnose prostate cancer which should ideally be nontoxic in vivo. Figure 7 showed that both the $[^{68}\text{Ga}]\text{Ga-PSMA-617}$ on its own and its ME formulated form were nontoxic to PC3 cell lines at concentrations lower than 0.0625 mg/mL. The PSMA-617 in the ME formulation serves as the ligand to the PSMA-617 receptor on the cell wall. The ME serves to alter the pharmacokinetics and delivery of the formulated PSMA-617. The in vitro cytotoxicity profile of the ME in the PC3 cell line showed that it had a similar effect as the $[^{68}\text{Ga}]\text{Ga}^{3+}$ alone, where the cell viability in the PC3 cell line was affected at concentrations of 0.0625 mg/mL and higher, the main aspect could be the composition of the ME resulted in acute toxicity to the cells. The ME therefore had a seemingly protective function towards the PC3 cell line, increasing the cell tolerance towards the $[^{68}\text{Ga}]\text{Ga}^{3+}$ at 0.0625 mg/mL or lower which could help it in serving the purpose of a diagnostic tool.

Only concentrations of $[^{68}\text{Ga}]\text{Ga}^{3+}$ (buffered with 2.5 M sodium acetate to pH 3.5) at 0.0625 mg/mL and higher inhibited cell growth of the PC3 prostate cancer cell line, comparable to what is seen in literature.²⁴ However, in combination with PSMA-617, the cell viability improved dramatically to more than 80% at all the concentrations except at 0.25 mg/mL which showed a significant measure of toxicity compared with the other concentrations used.

The $[^{68}\text{Ga}]\text{Ga}^{3+}$ was eluted as $[^{68}\text{Ga}]\text{GaCl}_3$ with 0.6 M HCl and buffered to pH 3.5 to 4 with NaOAc. The presence of the chloride ions and its acidic property may have rendered ≥ 0.0625 mg/mL of the $[^{68}\text{Ga}]\text{Ga}^{3+}$ concentrations toxic to the PC3 prostate cancer cell line. $[^{68}\text{Ga}]\text{Ga}^{3+}$ is a decay product of $[^{68}\text{Ge}]\text{Ge}^{4-}$ which in turn decays to zinc-68 (^{68}Zn) which is a nonradioactive isotope. Given the short half-life of $[^{68}\text{Ga}]\text{Ga}^{3+}$, the graph data is more a representation of decayed $[^{68}\text{Ga}]\text{Ga}^{3+}$, ie, ^{68}Zn which may be toxic to cells at high concentrations or doses. Zinc at low concentrations, on the other hand, plays a vital role in cell division and cell growth. This could be a possible explanation for the proliferated cell growth in all the test compounds containing $[^{68}\text{Ga}]\text{Ga}^{3+}$ at the lower concentration ranges.^{24, 25} Zinc also assists in the release of testosterone and insulin-like growth factor-1 (IGF-1), which build muscle mass and a healthy metabolism.²⁶ The addition of $[^{68}\text{Ga}]\text{Ga}^{3+}$ to either ME and/or in combination with PSMA-617 appeared to proliferate PC3 cell growth when compared with that in Figure 6. The $[^{68}\text{Ga}]\text{Ga}$ -PSMA-617 loaded ME was nontoxic to PSMA-positive PC3 cell lines at very low concentrations.

When the PSMA-617 and the ME were tested against the HEK 293 cells, several observations were made. The results in Figure 8 showed that the PSMA-617-ME formulations inhibited the growth of HEK 293 cells substantially and showed to be mildly toxic even at lower concentrations. A blank ME however presented low toxicity towards the cells at concentrations < 0.0625 mg/mL. Free PSMA-617 did not show concentration-dependent toxicities towards the cells. Concentrations of PSMA-617 below 0.015 mg/mL and above 0.5 mg/mL showed toxicity towards the cells. A similar trend albeit less prominent was also observed in PC3 cells.²⁷ The viability of all three test compounds, ME, PSMA, and PSMA-617-ME in Figure 8 against HEK 293 cells, was $< 40\%$ at a high concentration of 1 mg/mL. The toxicity profile of PSMA to HEK293 cells did not show a classical sigmoidal response in the concentration range tested. The ME on its own however proliferated cell growth (< 0.125 mg/mL) in both cell lines. Concentrations of $[^{68}\text{Ga}]\text{Ga}$ -PSMA-617-ME ≥ 0.0078 mg/mL may have induced cell death as a result of early or late stage apoptosis and cell nuclear morphology.²⁸ Toxicity of the ME may be influenced by particle properties (particle chemistry, mass, surface area, size, state of aggregation, and structure).²⁸ The low cell viability may be a result of dose and time-dependent cytotoxicity associated with cellular necrosis and apoptosis.²⁸ The combination of $[^{68}\text{Ga}]\text{Ga}^{3+}$ and PSMA-617 had a synergistic effect on cell proliferation which in part may be due to the cell growth properties of ^{68}Zn , the decay product of $[^{68}\text{Ga}]\text{Ga}^{3+}$ which probably acted as a nutritional supplement to the cell line.²⁴

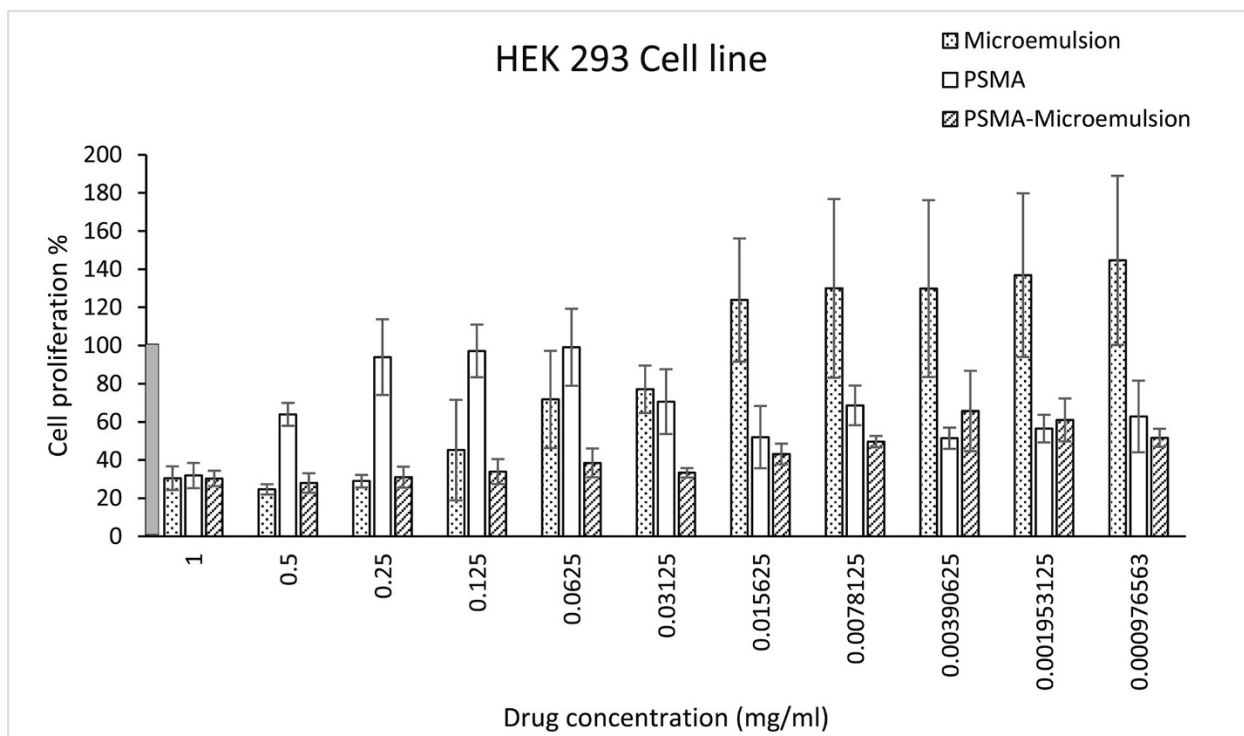


Figure 8. The in vitro cytotoxicity of a blank ME, PSMA-617, and PSMA-617-ME against HEK 293 cells after 24 h (n = 9). Grey bar represents the untreated control cells

Figure 9 depicts enhanced cell growth of HEK 293 cells treated with $[^{68}\text{Ga}]\text{Ga}^{3+}$ in combination with PSMA-617 and ME formulation. $[^{68}\text{Ga}]\text{Ga}$ -PSMA-617 did not appear to be toxic at all to the concentrations of the test compound, showing cell proliferation beyond 90%. $[^{68}\text{Ga}]\text{Ga}$ -PSMA-617-ME did not indicate cell toxicity at concentrations lower than 0.125 mg/mL and only showed moderate toxicity at higher concentrations. $[^{68}\text{Ga}]\text{Ga}^{3+}$ on its own, however, inhibited cell growth at concentrations ≥ 0.125 mg/mL. Figure 9 showed that both the $[^{68}\text{Ga}]\text{Ga}$ -PSMA-617 on its own and its formulated form in a ME showed little toxicity towards the HEK293 cells. This information could be advantageous, when considering the safety or toxicity of the diagnostic $[^{68}\text{Ga}]\text{Ga}$ -PSMA-617 radiopharmaceutical in PSMA-receptor-negative cells.

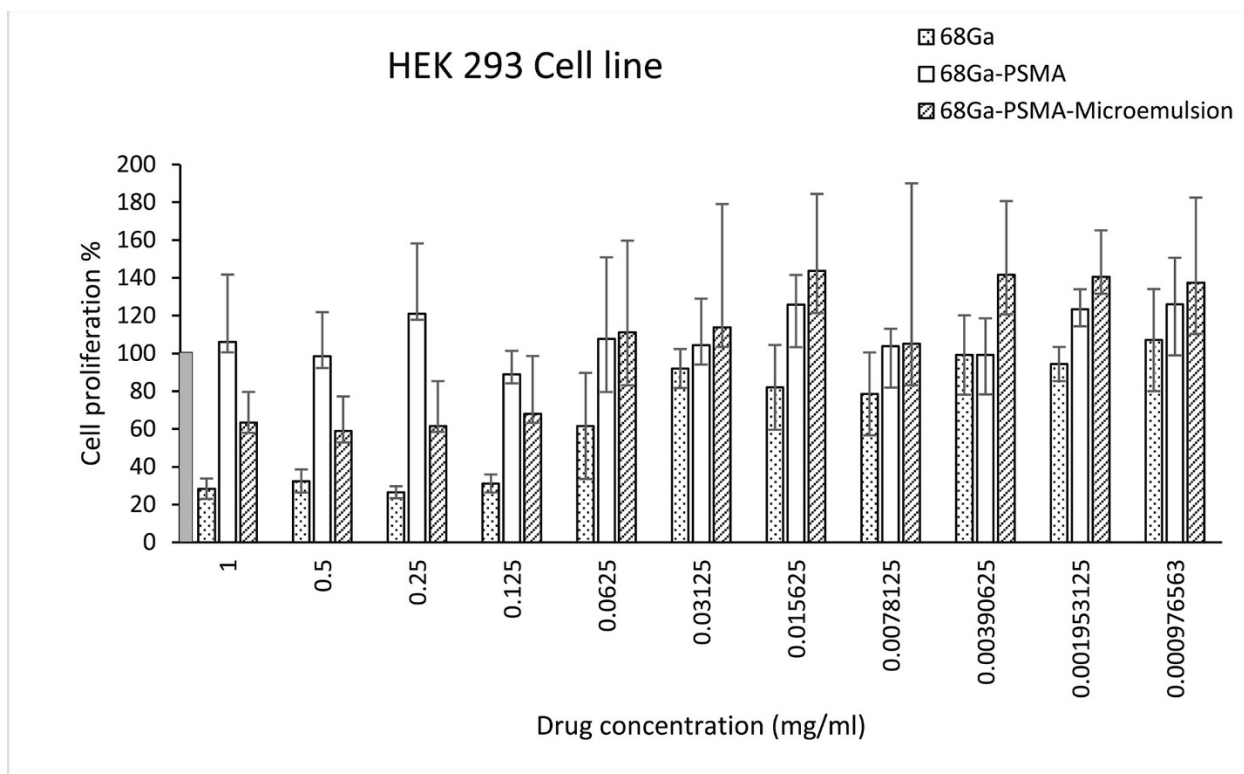


Figure 9. The cytotoxicity of $[^{68}\text{Ga}]\text{Ga}^{3+}$, $[^{68}\text{Ga}]\text{Ga-PSMA-617}$, and $[^{68}\text{Ga}]\text{Ga-PSMA-617-ME}$ against HEK 293 cell lines after a 24-h incubation ($n = 9$). Grey bar represents the untreated control cells

3.4 MicroPET/CT imaging and biodistribution of $[^{68}\text{Ga}]\text{Ga-PSMA-617-ME}$

To investigate the biodistribution pathway of $[^{68}\text{Ga}]\text{Ga-PSMA-617}$ (0.5-5 nmol) formulated ME, the test compound $[^{68}\text{Ga}]\text{Ga-PSMA-617-ME}$ was injected into the tail vein of healthy BALB/c mice. The injected radioactivity across all the mice was in the range of 0.76 to 13.96 MBq. Several mice ($n = 4$) were employed in the ex vivo biodistribution study only where low doses were sufficient for data acquisition and quantification. The 0.76 ± 0.24 MBq and 13.96 ± 0.22 MBq were the lowest and highest injected radioactivity, whereas an average dose of 5.89 ± 0.64 MBq was administered into mice for the microPET/CT imaging study.

Postadministration of the $[^{68}\text{Ga}]\text{Ga-PSMA-617-ME}$, biodistribution analysis resulted in mainly the excretory organs, viz. the kidneys shown in Figure 10. The kidneys had an average radioactivity of 31.33%ID/g followed by the small intestine (9.71%ID/g) and stomach (8.83%ID/g). Clearance into the small and large intestine will be via the biliary excretion route. This is expected from a formulation consisting of fatty acids. The highest trace amount of $[^{68}\text{Ga}]\text{Ga-PSMA-617-ME}$ was reported in the left kidney and the lowest in the brain (0.49%ID/g). Time activity clearance curves indicated that as early as 5 minutes after IV injection (as shown in Figure 11), there is clearance from the blood pool into the kidney and out via the urine in the bladder. The results in this study show a SUV (%ID/mL) for the bladder of 10 already by 30 minutes. Benešová et al² reported for

[⁶⁸Ga]Ga-PSMA-617 a SUV of 6 by 30 minutes only reaching 10 by 60 minutes. The SUV for kidneys are also higher, a peak of 5 at 15 minutes before tailoring off. In this study, the kidneys peak at 5 minutes with a SUV of 3. This may indicate that the kidney retention is lowered by the ME. From the biodistribution data in Figure 10, clearance into the small and large intestine will be via the biliary excretion route. This is expected from a formulation consisting of fatty acids. The found %ID/g for these two organs is elevated if compared with the [⁶⁸Ga]Ga-PSMA-617 alone.² This would also indicate that the ME does indeed alter the biodistribution of the [⁶⁸Ga]Ga-PSMA-617 providing some evidence that it may assist in reducing the side effects associated with [⁶⁸Ga]Ga-PSMA-617's solely urinary excretion pathway. This needs to be proven in a head-to-head study [⁶⁸Ga]Ga-PSMA-617-ME vs [⁶⁸Ga]Ga-PSMA-617 in tumour-bearing mice.

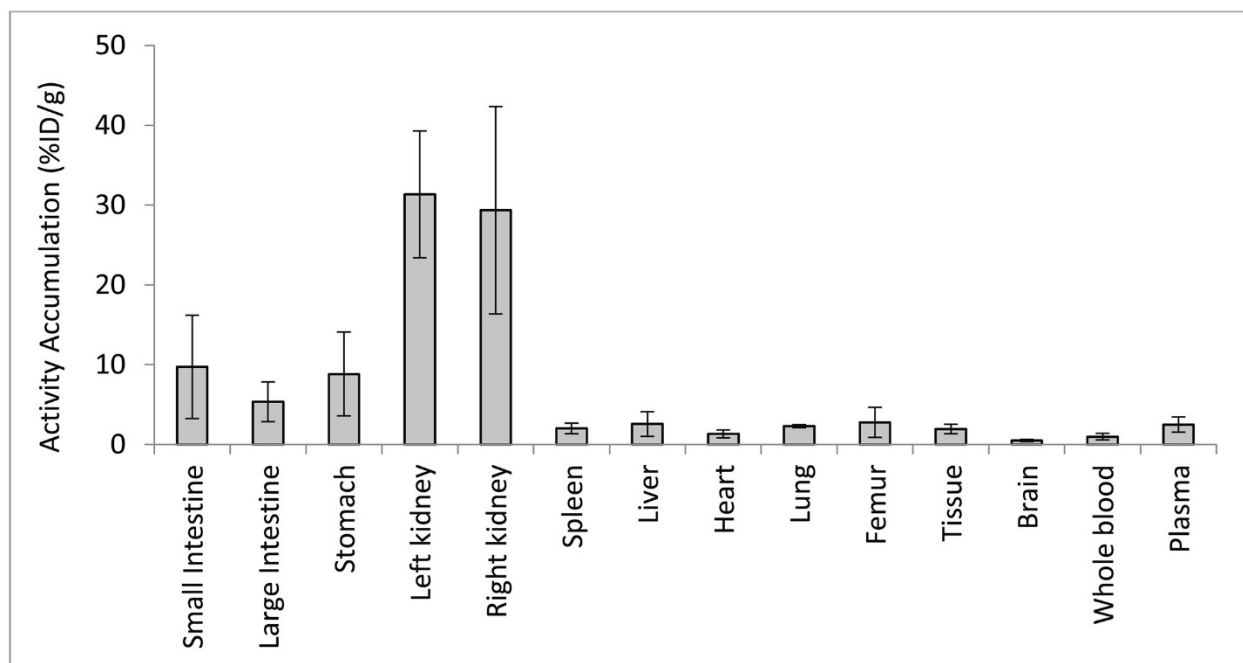


Figure 10. Relative organ biodistribution (%ID/g) analysed ex vivo 60 min after intravenous injection of [⁶⁸Ga]Ga-PSMA-617-ME. Results are expressed as mean ± SD (n = 4)

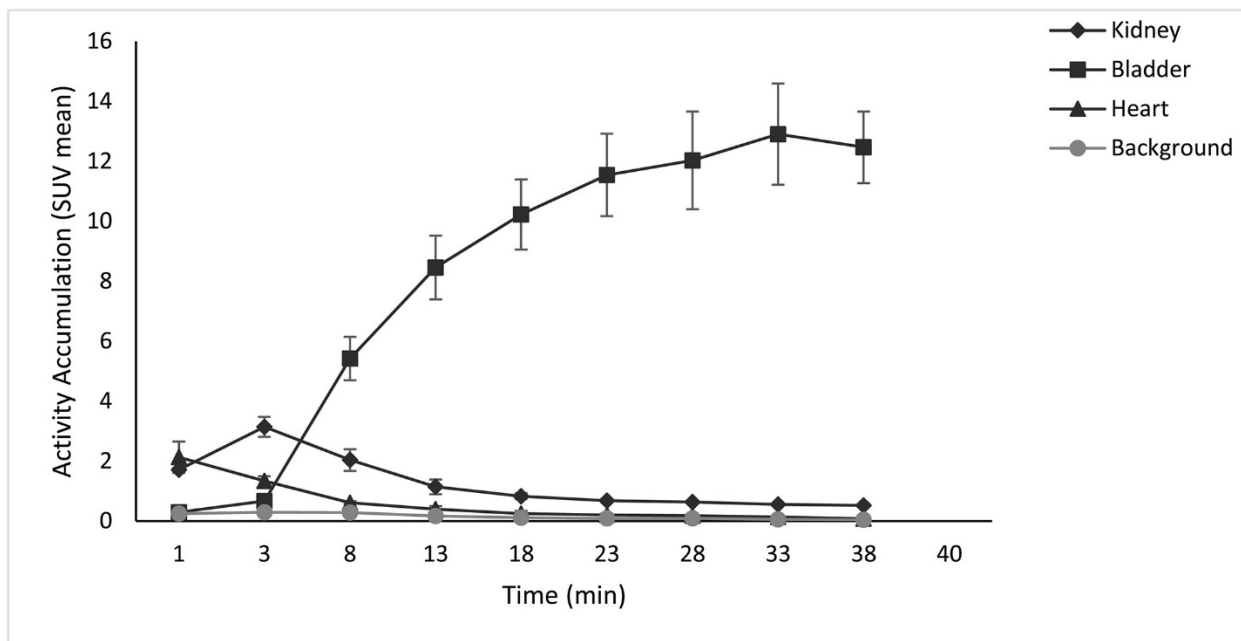


Figure 11. Time activity curve plot for blood pool (heart), kidney, and bladder derived from 40-min flow dynamic small animal microPET data of [^{68}Ga]Ga-PSMA-617-ME. Results are expressed as mean standardised uptake value (SUV mean) \pm SD (n = 4)

The highest radioactivity uptake was observed in the kidneys at 2.85%ID/mL at 3 minutes post IV injection and decreased to 1.01%ID/mL after 10 minutes. The radioactivity subsequently accumulated in the bladder, peaking to a maximum of 12.45%ID/mL after 38 minutes as depicted in Figure 11. In literature, PSMA-617 was found in other organs, such as the proximal renal tubules and salivary glands.¹³ This means that when [^{68}Ga]Ga-PSMA-617 is used as a target for radionuclide therapy, there will be a radiation dose delivered to these organs although at reduced doses as compared with prostate cancer cells.^{4, 13} This impacts the safe dose and side effect profile of PSMA-targeted therapy because ultimately significant radiation damage to nontarget organs needs to be avoided. Renal uptake of [^{68}Ga]Ga-PSMA-617 is partially due to the route of excretion of the agent and due to specific uptake from the expression of PSMA-617 in mouse proximal renal tubules.¹² The observation of high kidney radioactivity and uptake depicted in Figure 11 indicated rapid renal clearance of the [^{68}Ga]Ga-PSMA-617-ME from the system and shows a classic clearance curve for radiopharmaceuticals with a much faster clearance through the kidney into the bladder than reported for [^{68}Ga]Ga-PSMA-617 alone.²

4 CONCLUSION

The physical and chemical characteristics of the optimised ME formulation validated the safety and toxicity aspects of the ME for both in vitro and in vivo experiments. The physical stability of the formulation remained constant even with the incorporation of [^{68}Ga]Ga-PSMA-617 radiopharmaceutical. In this article, [^{68}Ga]Ga-PSMA-617 was successfully synthesised at a high radiochemical yield under determined conditions. The

radiopharmaceutical [⁶⁸Ga]Ga-PSMA-617 was incorporated into a ME formulation. Additionally, in vitro cytotoxicity studies revealed that a [⁶⁸Ga]Ga-PSMA-617–loaded ME was nontoxic to both PSMA-positive PC3 and PSMA-negative HEK 293 cell lines at 0.0625 mg/mL or lower, therefore allowing its evaluation as a delivery system for [⁶⁸Ga]Ga-PSMA-617 diagnostic studies. The [⁶⁸Ga]Ga-PSMA-617–loaded ME followed the typical enterohepatic metabolism of [⁶⁸Ga]Ga-PSMA-617, with rapid excretion from the blood pool with some biliary clearance into the (small and large) intestines which was elevated above the reported values for [⁶⁸Ga]Ga-PSMA-617 alone. This also indicates that there was also no in vivo toxicity observed and no concerns raised by the biodistribution data. This paves the way for further studies in tumour-bearing animals to prove that the ME sufficiently enough alters the biodistribution of [⁶⁸Ga]Ga-PSMA-617 so that it offers the slower release of radiopharmaceuticals from the circulation but not retained by the kidneys for long periods of time when excreted thereby improving their overall tumour uptake and reducing the renal radiation burden.

ACKNOWLEDGEMENTS

The authors would like to thank and acknowledge the Nuclear Technologies in Medicine and the Biosciences Initiative (NTEMBI), a national technology platform developed and managed by the South African Nuclear Energy Corporation (Necsa) and funded by the Department of Science and Technology (DST). The authors would like to thank the Department of Nuclear Medicine at the University of Pretoria and the Council for Scientific and Industrial Research (CSIR) for resources provided. The authors thank Delene van Wyk for the image analysis and Janie Duvenhage for assistance with the biodistribution determination. The authors would also like to thank Biljana Marjanovic-Painter for the HPLC analysis, as well as Kobus Venter and Cor Bester from the North West University for assistance with the animal studies. A special thank you to the Carl and Emily Fuchs Foundation for assisting in funding this project.

REFERENCES

¹Zhu H, Xie Q, Li N, Tian H, Liu F, Yang Z. Radio-synthesis and mass spectrometry analysis of ⁶⁸Ga-DKFZ- PSMA-617 for non-invasive prostate cancer PET imaging. *J Radioanal Nucl Chem Springer Netherlands*. 2016; **309**(2): 575- 581.

²Benešová M, Schäfer M, Bauder-Wüst U, et al. Preclinical evaluation of a tailor-made DOTA-conjugated PSMA inhibitor with optimized linker moiety for imaging and endoradiotherapy of prostate cancer. *J Nucl Med*. 2015; **56**(6): 914- 920.

³ Prostate cancer statistics. World Cancer Research Fund International 2017 November 24. Available from: <http://www.wcrf.org/int/cancer-facts-figures/data-specific-cancers/prostate-cancer-statistics>.

⁴Xu J, Yu J, Xu X, et al. Evaluation of PSMA-targeted glycol chitosan micelles for prostate cancer therapy. *J Nanomat*. 2014; 2014; 158.

- ⁵Afshar-Oromieh A, Avtzi E, Giesel FL, et al. The diagnostic value of PET/CT imaging with the ⁶⁸Ga-labelled PSMA ligand HBED-CC in the diagnosis of recurrent prostate cancer. *Eur J Nucl Med Mol Imaging*. 2014; **42**(2): 197- 209.
- ⁶Afshar-Oromieh A, Hetzheim H, Kratochwil C, et al. The novel theranostic PSMA-ligand PSMA-617 in the diagnosis of prostate cancer by PET/CT: biodistribution in humans, radiation dosimetry and first evaluation of tumor lesions. *J Nucl Med*. 2015; **56**(11): 1697- 1705. jnumed.115.161299-. Available from: <http://jnm.snmjournals.org/content/early/2015/08/19/jnumed.115.161299papetoc>
- ⁷Eder M, Neels O, Müller M, et al. Novel preclinical and radiopharmaceutical aspects of [⁶⁸Ga]Ga-PSMA-HBED-CC: a new PET tracer for imaging of prostate cancer. *Pharmaceuticals*. 2014; **7**(7): 779- 796.
- ⁸Herrmann K, Bluemel C, Weineisen M, et al. Biodistribution and radiation dosimetry for a novel probe targeting prostate specific membrane antigen for imaging and therapy (⁶⁸Ga-PSMA I&T). *J Nucl Med*. 2015; **56**(6): 1- 24. Available from: <https://doi-org.uplib.idm.oclc.org/10.2967/jnumed.115.156133>
- ⁹Nedrow JR, Latoche JD, Day KE, et al. Targeting PSMA with a Cu-64 labeled phosphoramidate inhibitor for PET/CT imaging of variant PSMA-expressing xenografts in mouse models of prostate cancer. *Mol Imaging Biol*. 2015; **18**(3): 402- 410.
- ¹⁰Weineisen M, Simecek J, Schottelius M, Schwaiger M, Wester H-J. Synthesis and preclinical evaluation of DOTAGA-conjugated PSMA ligands for functional imaging and endoradiotherapy of prostate cancer. *EJNMMI Res*. 2014; **4**(1): 1- 15. Available from: <http://www.ejnmmires.com/content/4/1/63>
- ¹¹Weineisen M, Schottelius M, Simecek J, et al. ⁶⁸Ga- and ¹⁷⁷Lu-labeled PSMA I&T: optimization of a PSMA-targeted theranostic concept and first proof-of-concept human studies. *J Nucl Med*. 2015; **56**(8): 1169- 1176. Available from: <http://www.ncbi.nlm.nih.gov.uplib.idm.oclc.org/pubmed/26089548>
- ¹²Wong P, Li L, Chea J, et al. PET imaging of ⁶⁴Cu-DOTA-scFv-anti-PSMA lipid nanoparticles (LNPs): enhanced tumor targeting over anti-PSMA scFv or untargeted LNPs. *Nucl Med Biol*. 2017; **47**: 62- 68. Available from: <https://doi-org.uplib.idm.oclc.org/10.1016/j.nucmedbio.2017.01.004>
- ¹³Melariri P, Kalombo L, Nkuna P, Dube A, Ogutu B, et al. Oral lipid-based nanoformulation of tafenoquine enhanced bioavailability and blood stage antimalarial efficacy and led to a reduction in human red blood cell loss in mice. *Int J Nanomedicine*. 2015; **10**: 1493- 1503.
- ¹⁴Muzaffar F, Singh UK, Chauhan L. Review on microemulsion as futuristic drug delivery. *Int J Pharm Pharm Sci*. 2013; **5**(3): 39- 53.
- ¹⁵Moghimpour E, Salimi A, Eftekhari S. Design and characterization of microemulsion systems for naproxen. *Adv Pharm Bull*. 2013; **3**(1): 63- 71.
- ¹⁶Emmett L, Willowson K, Violet J, Shin J, Blanksby A, Lee J. Lutetium-177 PSMA radionuclide therapy for men with prostate cancer: a review of the current literature and discussion of practical aspects of therapy. *J Med Rad Sci*. 2017; **64**(1): 52- 60.
- ¹⁷Breeman WAP, de Jong M, de Blois E, Bernard BF, Konijnenberg M, Krenning EP. Radiolabelling DOTA-peptides with ⁶⁸Ga. *Eur J Nucl Med Mol Imaging*. 2005; **32**(4): 478- 485.

- ¹⁸Umbricht CA, Bene M, Schmid RM, et al. Sc-PSMA-617 for radiotheragnostics in tandem with ¹⁷⁷Lu-PSMA-617- preclinical investigations in comparison with ⁶⁸Ga-PSMA-11 and ⁶⁸Ga-PSMA-617. *EJNMMI*. 2017; **7**(9): 1- 10.
- ¹⁹Ebenhan T, Vorster M, Marjanovic-Painter B, et al. Development of a single vial kit solution for radiolabeling of ⁶⁸Ga-DKFZ-PSMA-11 and its performance in prostate cancer patients. *Molecules*. 2015; **20**(8): 14860- 14878.
- ²⁰Mokaleng BB, Ebenhan T, Ramesh S, et al. Synthesis, ⁶⁸Ga-radiolabeling and preliminary *in vivo* assessment of a depsipeptide-derived compound as a potential PET/CT infection imaging agent. *Biomed Res Int*. 2015; **2015**:284354. <https://doi-org.uplib.idm.oclc.org/10.1155/2015/284354>
- ²¹Parhi R, Suresh P. Preparation and characterization of solid lipid nanoparticles—a review. *Curr Drug Discov Technol*. 2012; **9**(1): 2- 16.
- ²²Baroli B, Lopez-quintela MA, Begona M, Fadda AM. Microemulsions for topical delivery of 8-methoxsalen. *J Control Release*. 2000; **69**(1): 209- 218.
- ²³Li Y, Maux S, Xiao H, McClements DJ. Emulsion based delivery systems for tributyrin, a potential colon cancer preventative agent. *J Agric Food Chem*. 2009; **57**(19): 9243- 9249.
- ²⁴Chitambar CR. Medical applications and toxicities of gallium compounds. *Int J Environ Res Public Health*. 2010; **7**(5): 2337- 2361.
- ²⁵Song Y, Ho E. Zinc and prostate cancer. *NIH Public Access*. 2009; **12**(6): 640- 645.
- ²⁶Wong P, Abubakar S. Comparative transcriptional study of the effects of high intracellular zinc on prostate carcinoma cells. *Oncol Rep*. 2010; **23**: 1501- 1516.
- ²⁷Yao V, Berkman CE, Choi JK, Keefe DSO, Bacich DJ. Expression of prostate-specific membrane antigen (PSMA), increases cell folate uptake and proliferation and suggests a novel role for PSMA in the uptake of the non-polyglutamated folate, folic acid. *Wiley Interscience*. 2009; 1- 12.
- ²⁸Selvaraj V, Bodapati S, Murray E, et al. Cytotoxicity and genotoxicity caused by yttrium oxide nanoparticles in HEK293 cells. *Int J Nanomedicine*. 2014; **9**: 1379- 1391.